

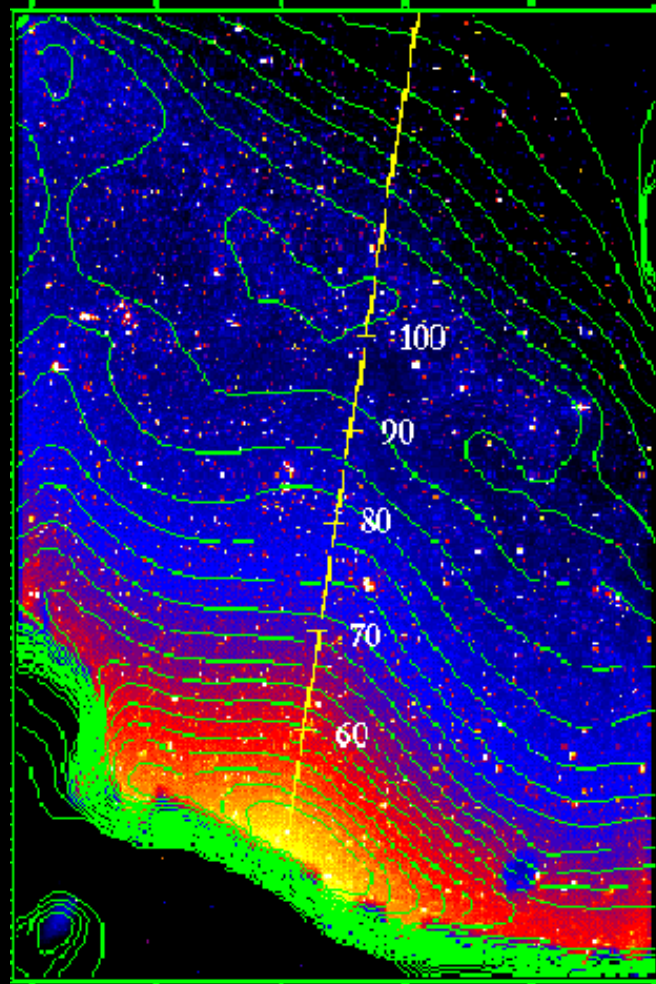
# 木曾シュミットを用いた 彗星ダスト雲の研究

石黒正晃（国立天文台→ソウル大学）

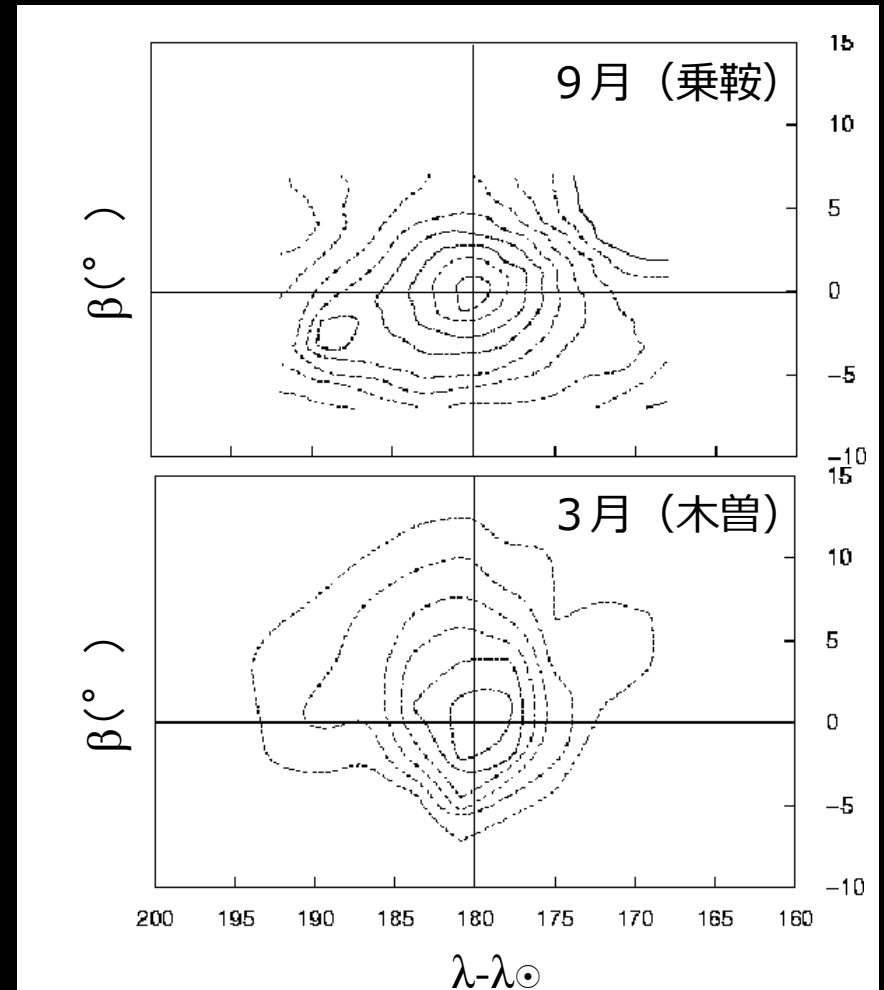
共同研究者

猿楽祐樹（木曾観測所）、渡部潤一（国立天文台）、  
上野宗孝、臼井文彦、大坪貴文（JAXA）、向井正（神戸大学）  
S. S. Hong、J. Pyo（ソウル大学）、S. M. Kwon（カンウォン大学）

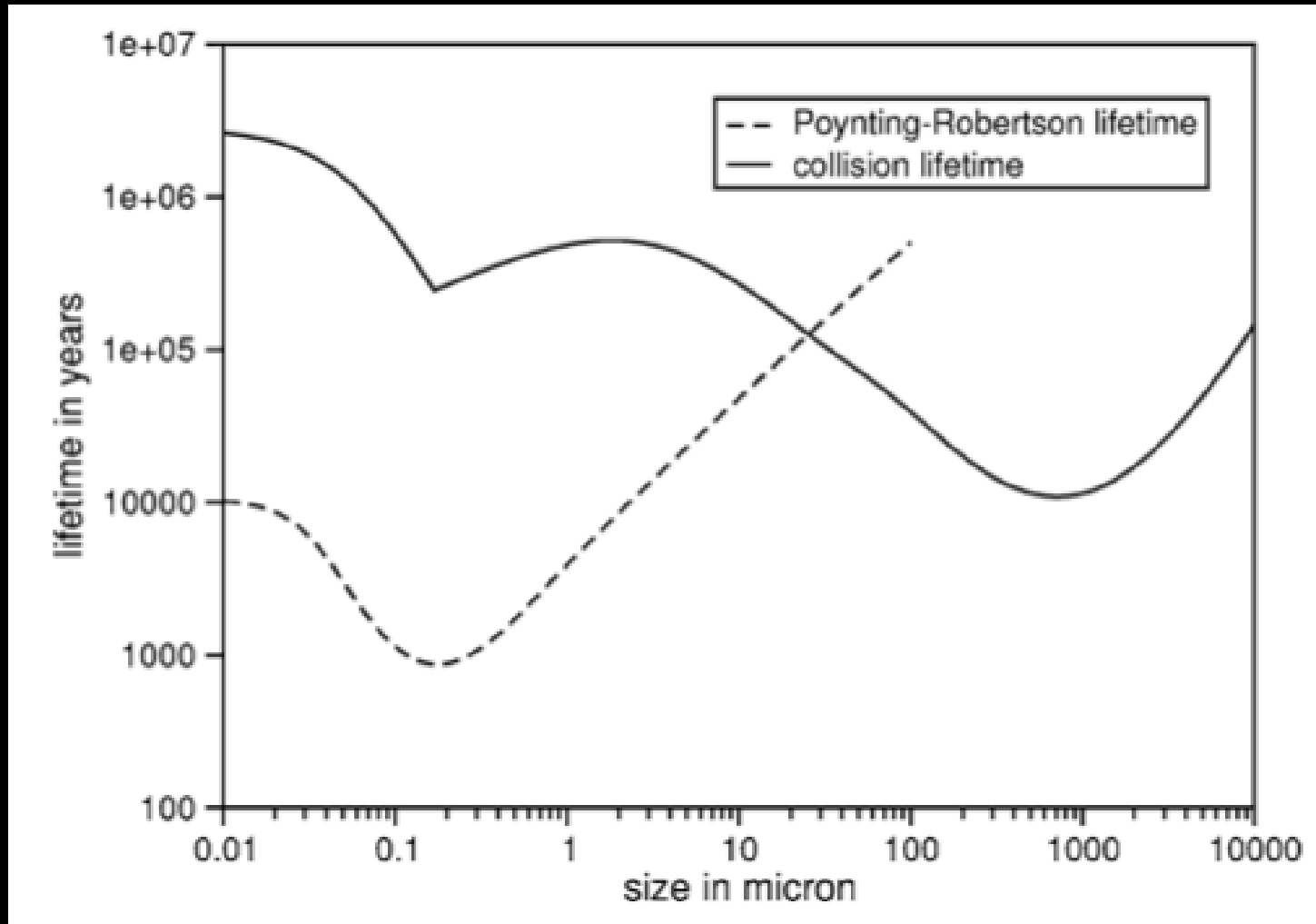
# 黄道光と対日照



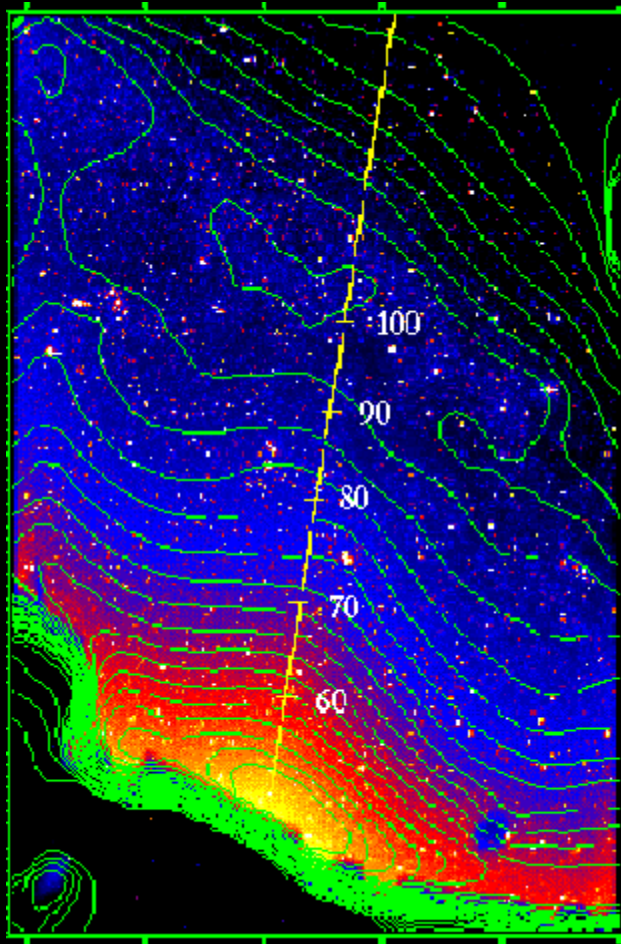
1997年3月5日 (木曾観測所)



# 黄道雲ダストの寿命



# 惑星間塵雲の起源に関する論争



惑星間塵は、毎秒約10トンの割合で失われている。

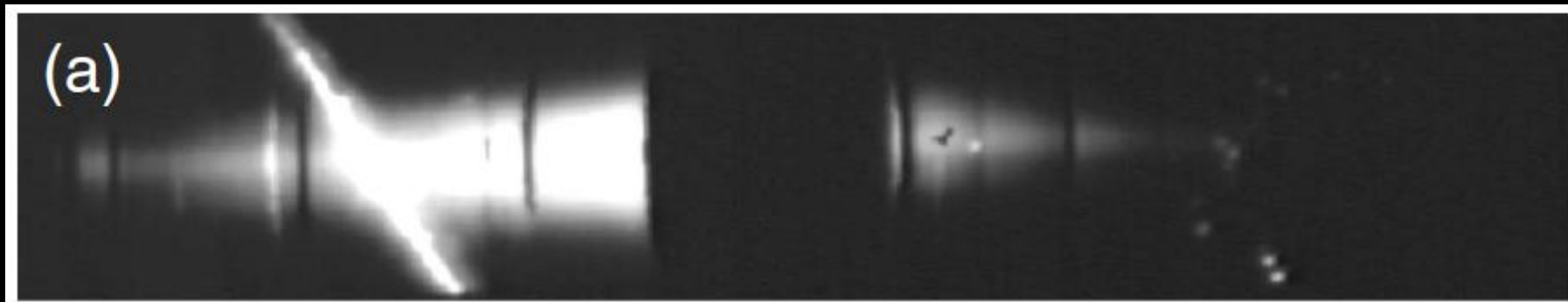
惑星間塵雲の起源として、

○彗星活動

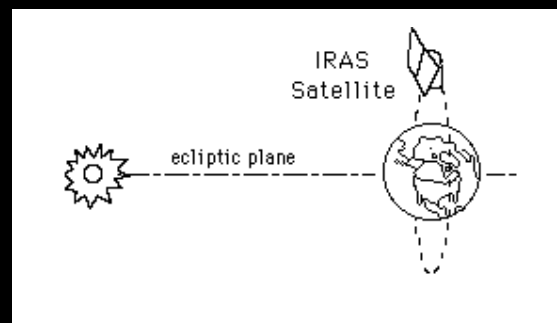
○小惑星同士の衝突

○星間ダストの流入

などが考えられる。

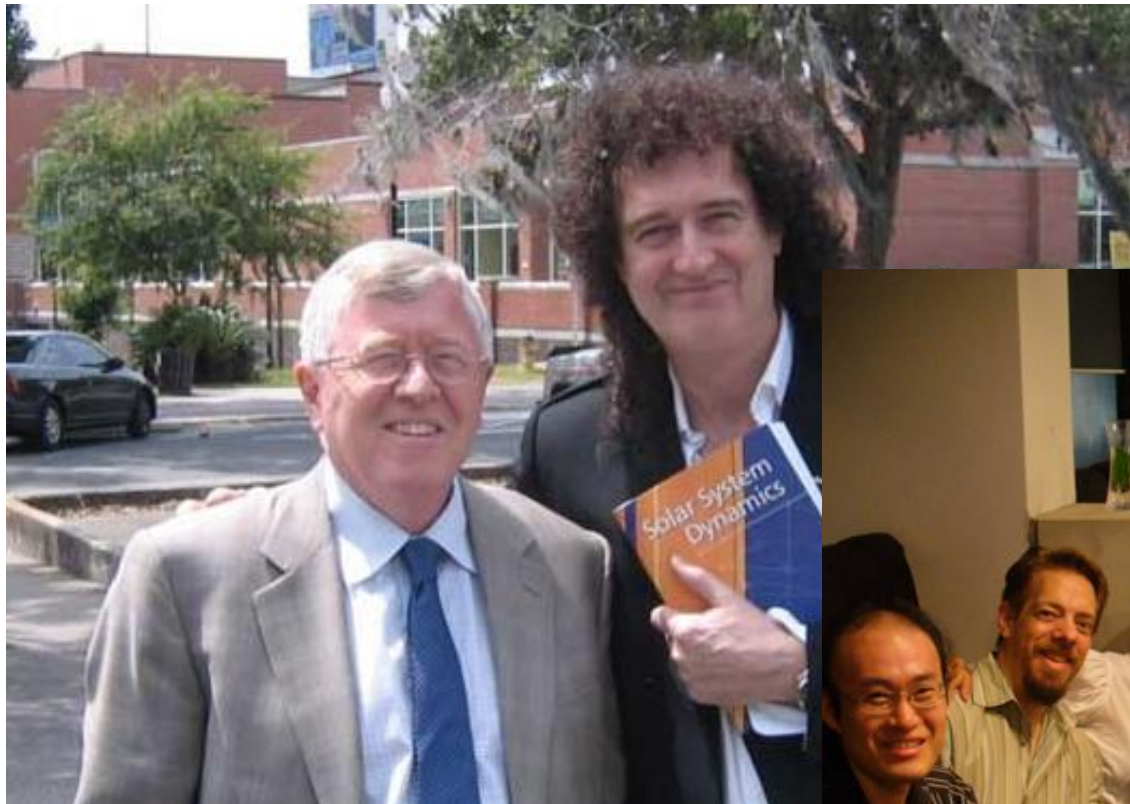


Courtesy of M. Sykes



# Mechanism of dust band production

## Equilibrium model vs Non-equilibrium model

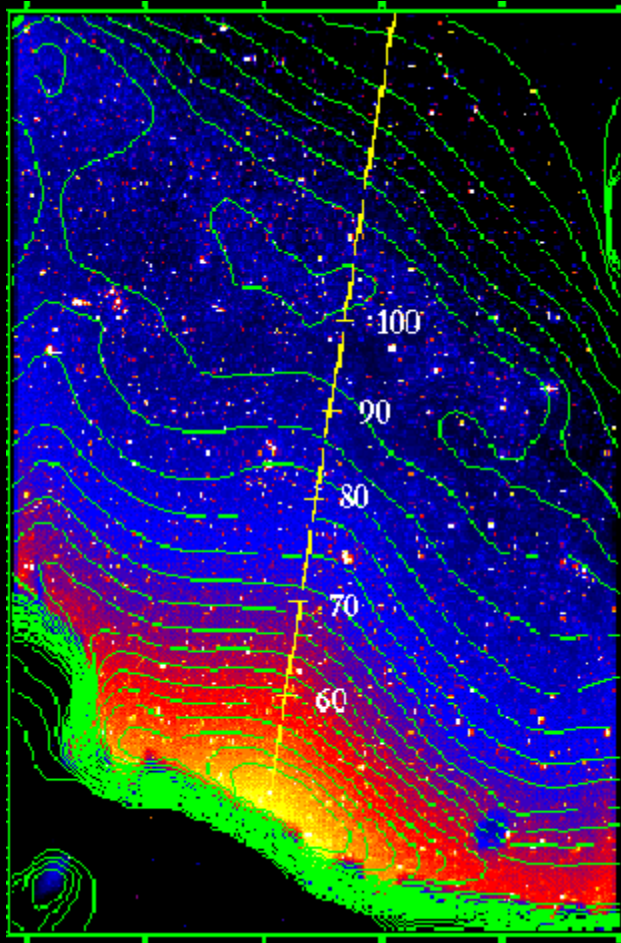


itudes of the bands appear to  
be most prominent Hirayama

bands. If this model is correct,  
related to known asteroid familie



# 2000年以前の起源に関する考察



小惑星ダストバンドの観測から、  
小惑星起源塵は黄道光の明るさの  
大半 ( $> 75\%$ ) に寄与している  
(e.g. Grogan et al. 1997)

彗星コマの明るさから、彗星起源  
塵の寄与は、無視できるくらい小  
さいと報告されている (Kresak &  
Kresakova 1987)

# IRAS Image of Cometary Dust Trail



Courtesy of Mark Sykes

# First Detection of Cometary Dust Trail by Kiso Schmidt



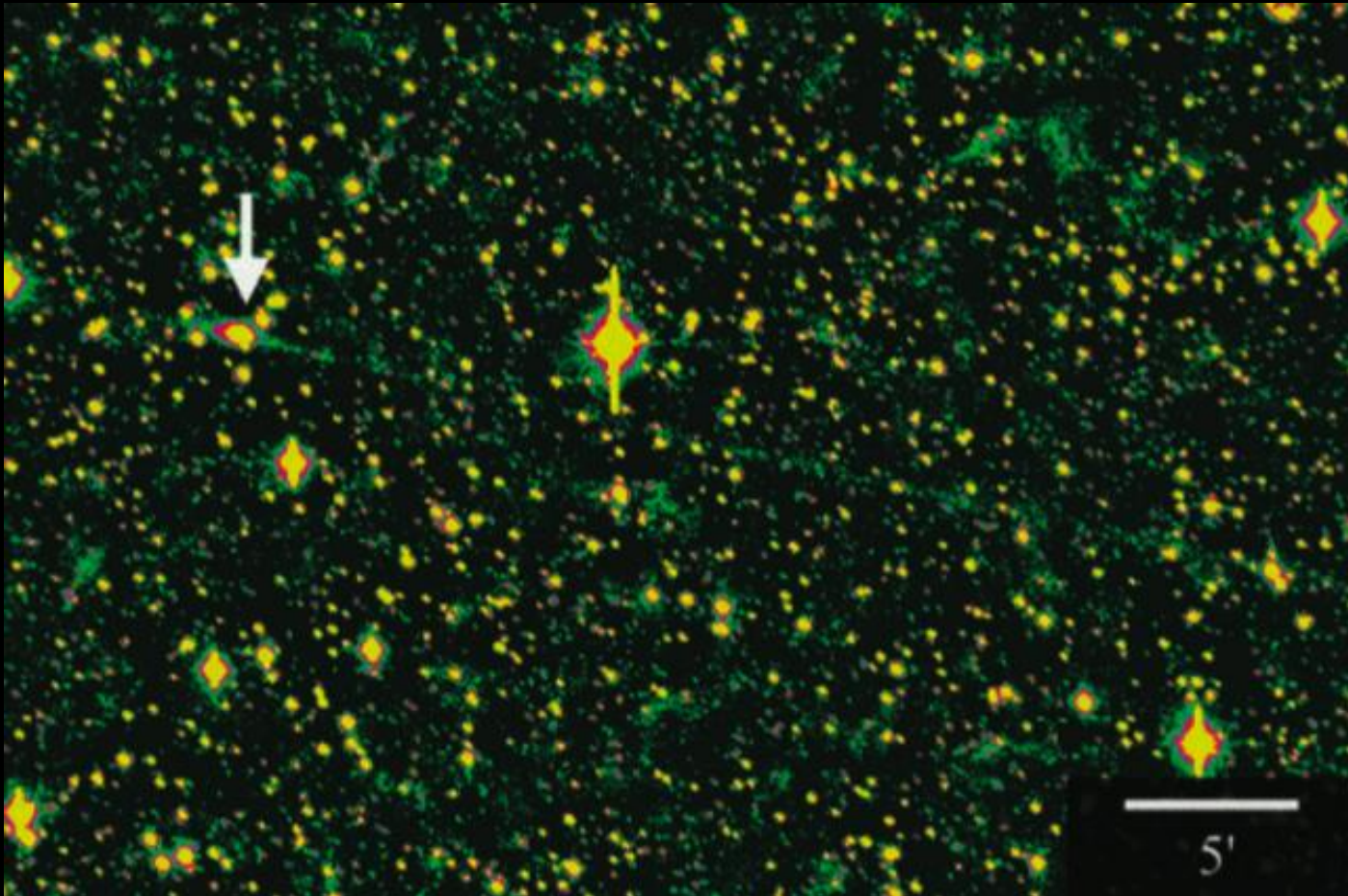
22P/Kopff

$R_h=3.01(\text{AU})$ ,  $\Delta=2.19(\text{AU})$

Feb. 15, 2002

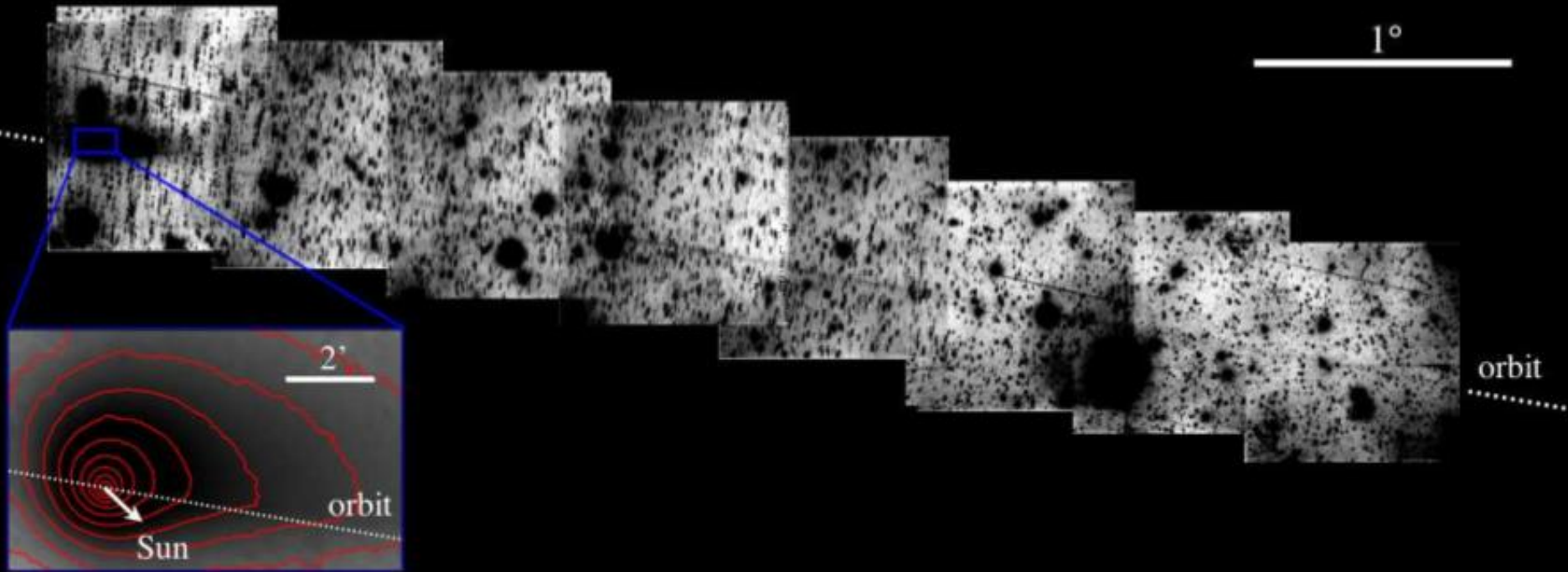
Ishiguro et al. 2002

# Wild Comet: Stardust Mission Target 81P/Wild 2



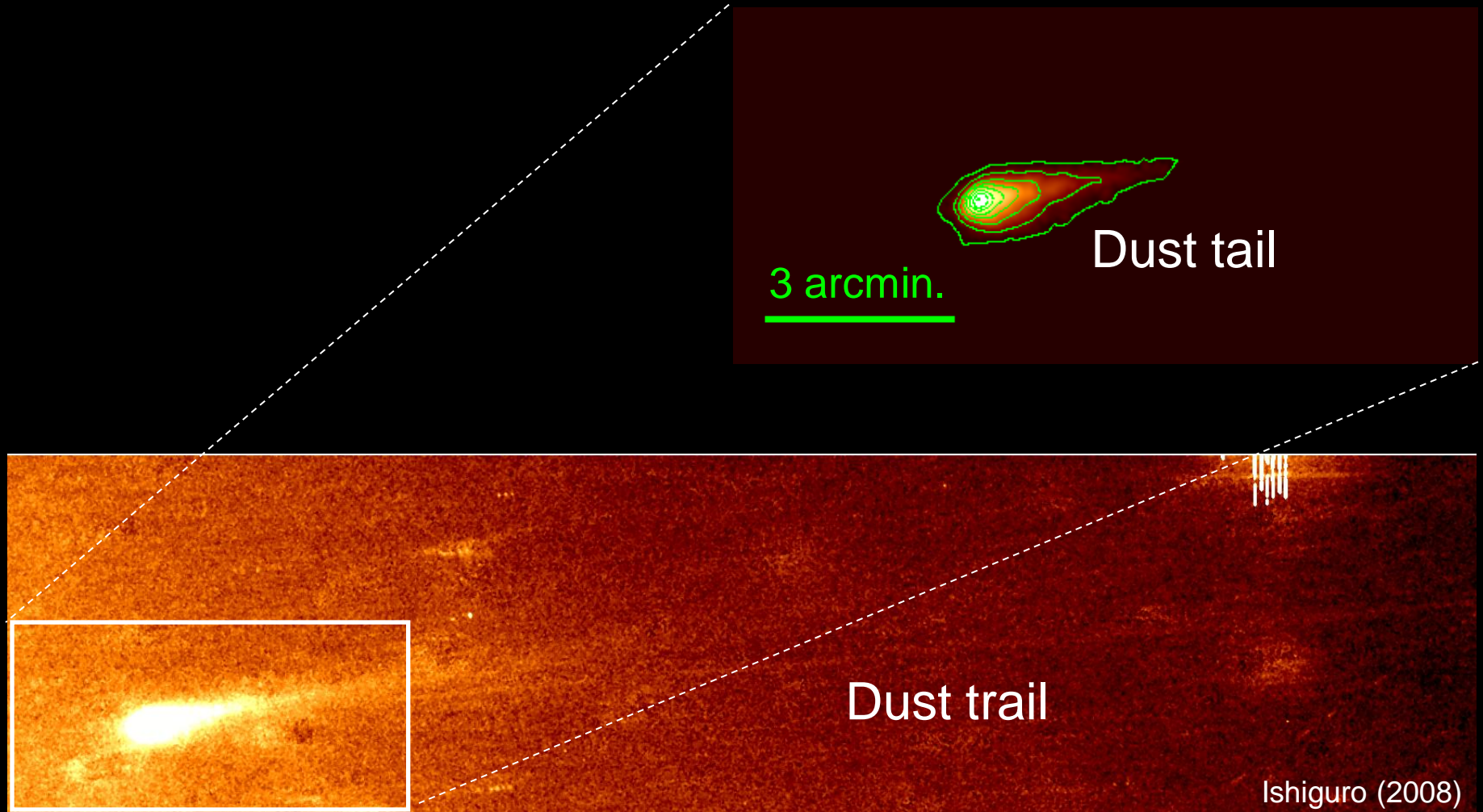
Ishiguro et al. 2003

# Long-extended ( $>10\text{deg}$ ) Dust Trail Associated with 4P/Faye



Sarugaku et al. 2007

# Rosetta Mission Target: 67P/Churyumov-Gerasimenko



# Model Description

## Dust Emission

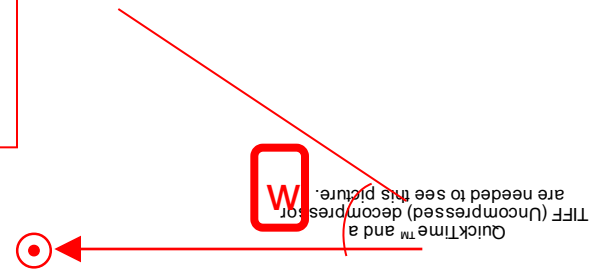
- Ejection velocity ( $r_h, a$ )
- Production rate ( $r_h, a$ )
- Width of cone-shape jet

$$v_{ej}(r_h, a) = V_0 \left( \frac{a}{a_0} \right)^{-u1} \left( \frac{r_h}{\text{AU}} \right)^{-u2}$$

$$N(a;t) da dt = \begin{cases} N_0 \left( \frac{r_h(t)}{\text{AU}} \right)^{-k} \left( \frac{a}{a_0} \right)^{-q} da dt \\ 0 \end{cases}$$

$$a_{min} \leq a \leq a_{max}$$

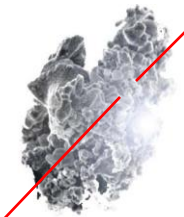
$$a < a_{min}, a > a_{max}$$



## Dynamical Evolution

- Solar gravity & radiation pressure
- ~~Planetary perturbations~~
- ~~Poynting-Robertson drag~~
- ~~Solar wind~~
- ~~Yarkovsky effect~~

Radiation pressure

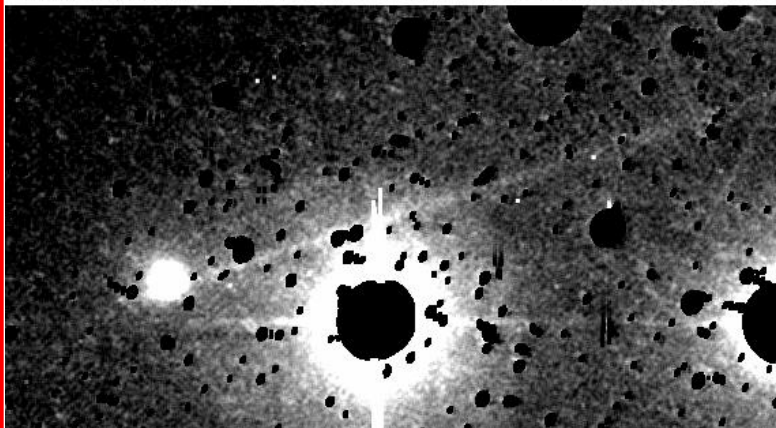
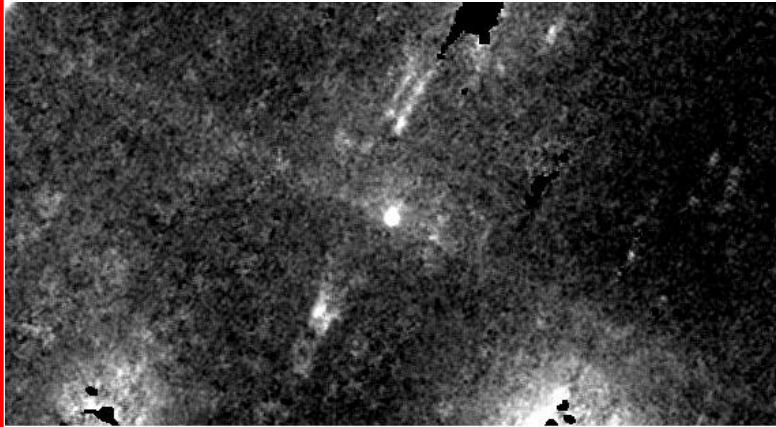


Solar gravity

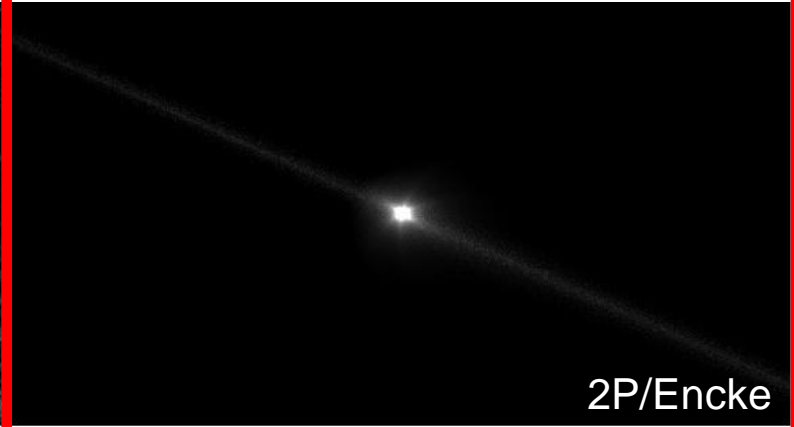


$$\beta \equiv \frac{F_r}{F_g} = \frac{KQ_{pr}}{\rho a}$$

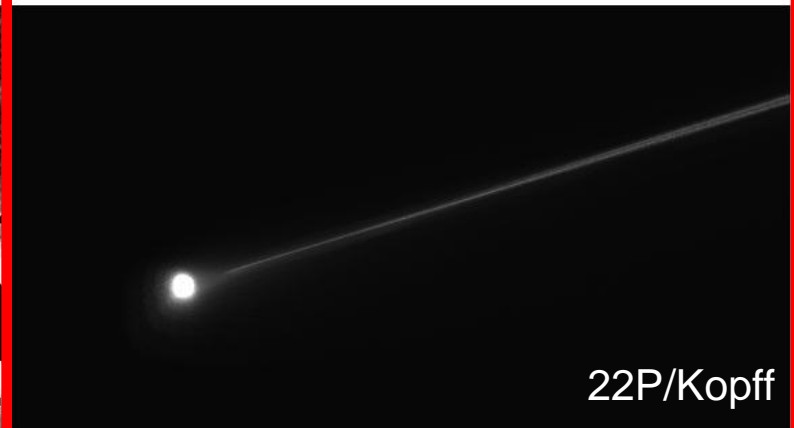
# OBSERVATIONS



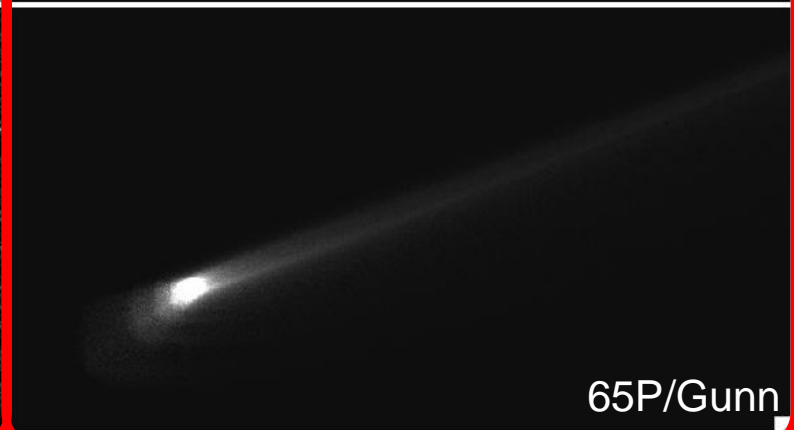
# MODEL



2P/Encke



22P/Kopff



65P/Gunn

# 彗星の質量供給率

comets	q [AU]	nucleus radius	$a_{MAX}$ [mm]	q	$V_{d=1mm}$ @q [m/s]	dM/dt [kg/s]	Ref.
2P/Encke	0.3	2.4-4.4	100	$3.25 \pm 0.25$	$5.5 \pm 2.8$	$48 \pm 20$	1
67P/Churyumov-Gerasimenko	1.3	1.3-2.5	5	$\sim 3.5$	$3.5 \pm 1.8$	$20 \pm 6$	3
22P/Kopff	1.6	1.7-2.5	10	$3.35 \pm 0.15$	$1.3 \pm 0.7$	$17 \pm 3$	1
4P/Faye	1.7	1.3-2.3	4.75	$3.5 \pm 0.1$	$1.2 \pm 0.6$	$20 \pm 6$	2
40P/Vaisala	1.8	1.5-1.8	2.5	$\sim 3.4$	$1.0 \pm 0.5$	$2.2 \pm 0.7$	4
118P/Shemaker-Levy 4	2.0	1.7-2.4	2	$\sim 3.2$	$1.7 \pm 0.9$	$8.3 \pm 2.5$	4
123P/West-Hartley	2.1	2.2	1	$\sim 3.2$	$1.5 \pm 0.8$	$7.3 \pm 2.2$	4
53P/Van Biesbroeck	2.4	3.3-3.9	3	$\sim 3.2$	$1.2 \pm 0.6$	$58 \pm 18$	4
65P/Gunn	2.5	$\sim 4.8$	1	$3.35 \pm 0.15$	$0.7 \pm 0.4$	$27 \pm 9$	1

## [References]

1. Ishiguro, Sarugaku, Ueno, Miura, Usui, Chun, Kwon Icarus **189**, 169 (2007)
2. Sarugaku, Ishiguro, Pyo, Miura, Nakada, Usui, Ueno, PASJ **59**, L25 (2007)
3. Ishiguro, Icarus **193**, 96 (2008)
4. This work

- It is found that the average mass-loss rate of 9 comets are 23 kg/s. **Our results is one order of magnitude higher than that of the previous studies for comae** (Kresák & Kresákobá 1987).
- At present there are about 200 short-period comets. Assuming that all of these comets inject the dust particles at the rate of 23 kg/s, **short-period comets can compensate half of mass lost** by Poynting-Robertson drag and mutual collision.
- Recent study of small asteroids suggest that the IRAS dust bands were generated by the catastrophic disruption events associated with young families (the Karin, the Veritas and Beagle families). According to an estimate by Nesvorny et al. (2007), the contribution of the dust particles responsible for IRAS dust bands is 10% or less of whole zodiacal cloud.

≈50 % from comets

<10 % from asteroids

# 査読論文リスト

Authors: Ishiguro, Sarugaku, Nishihara, Nakada, Nishiura, Soyano, Tarusawa, Mukai, Kwon, Hasegawa, Usui, Ueno  
Title: Report on the Kiso cometary dust trail survey  
Journal: Advances in Space Research, Volume 43, Issue 5, p. 875-879.

Authors: Ishiguro, M.  
Title: Cometary Dust Trail Associated with Rosetta Mission Target: 67P/Churyumov-Gerasimenko  
Journal: Icarus 193, 96-104, 2008

Authors: Sarugaku, Y., Ishiguro, M., Pyo, J. H., Miura, N., Nakada, Y., Usui, F., Ueno, M.  
Title: Detection of Long-Extended Dust Trail Associated with Short Period Comet 4P/Faye in 2006 Return  
Journal: Publication of the Astronomical Society of Japan 59, No. 4, L25-L28, 2007

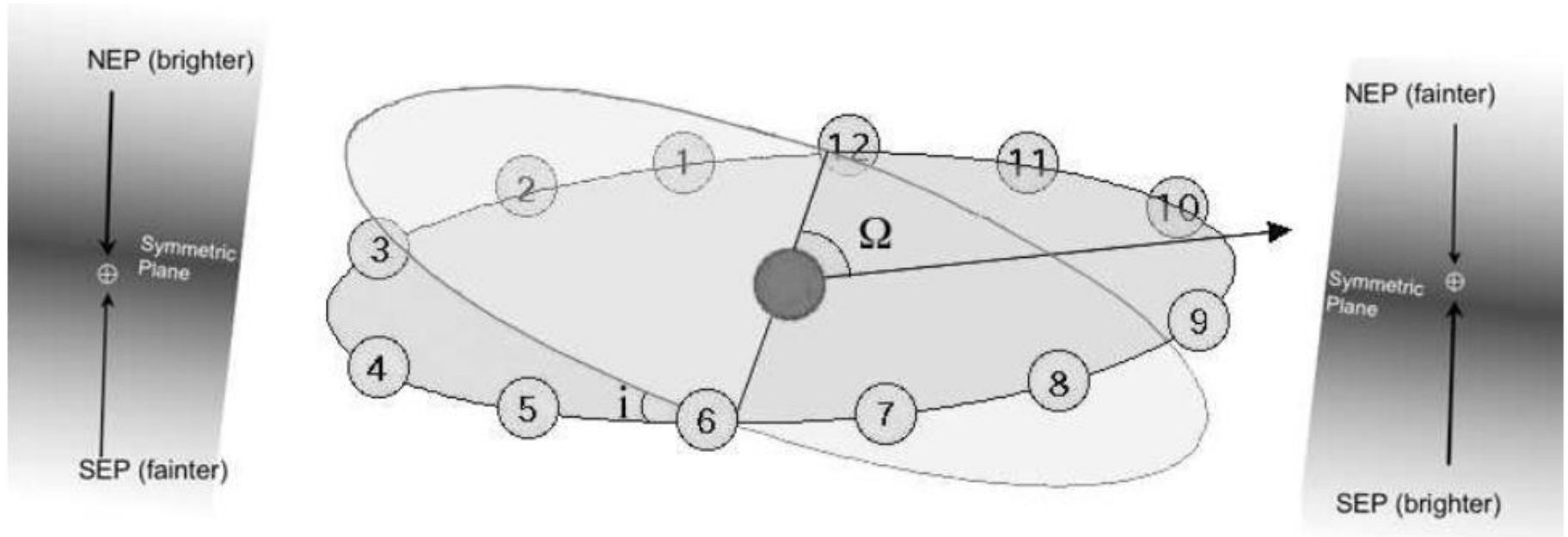
Authors: Ishiguro, M., Sarugaku, Y., Ueno, M., Miura, N., Usui, F., Chun, M. Y., Kwon, S. M.  
Title: Dark Red Debris from Three Short-Period Comets: P/Encke, 22P/Kopff, and 65P/Gunn  
Journal: Icarus 189, 169-183, 2007

Authors: Ishiguro, M., Kwon, S. M., Sarugaku, Y., Hasegawa, S., Usui, F., Nishiura, S., Nakada, Y., Yano, H.  
Title: Discovery of the Dust Trail of the Stardust Comet Sample Return Mission Target: 81P/Wild 2  
Journal: Astrophysical Journal 589, L101-L104, 2003

Authors: Ishiguro, M., Watanabe, J., Usui, F., Tanigawa, T., Kinoshita, D., Suzuki, J., Nakamura, R., Ueno, M., Mukai, T.  
Title: First Detection of an Optical Dust Trail along the Orbit of 22P/Kopff  
Journal: Astrophysical Journal 572, L117-L120, 2002





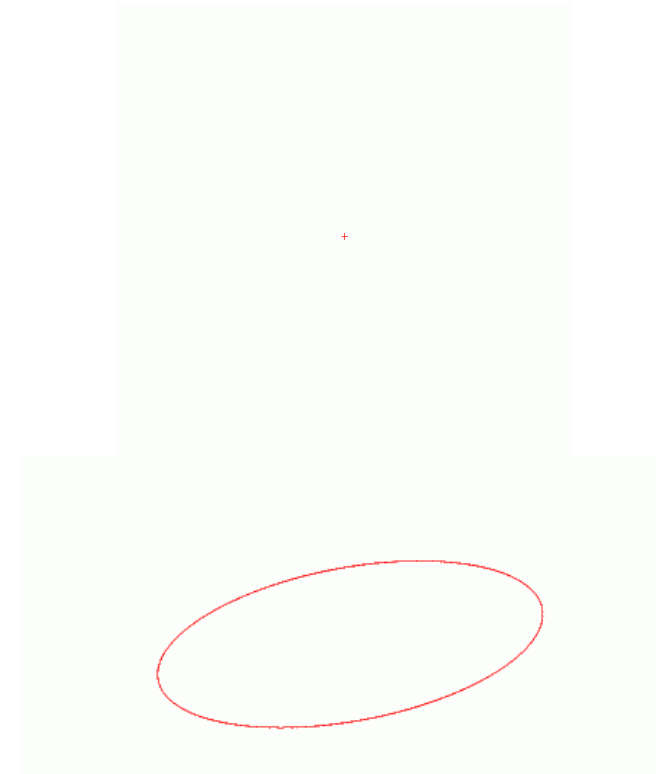
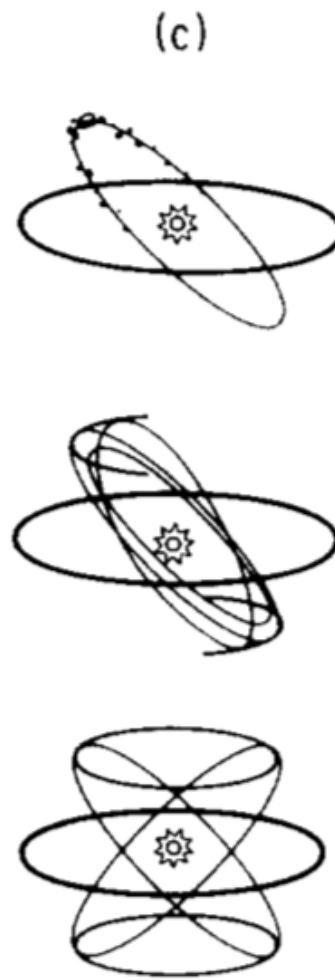
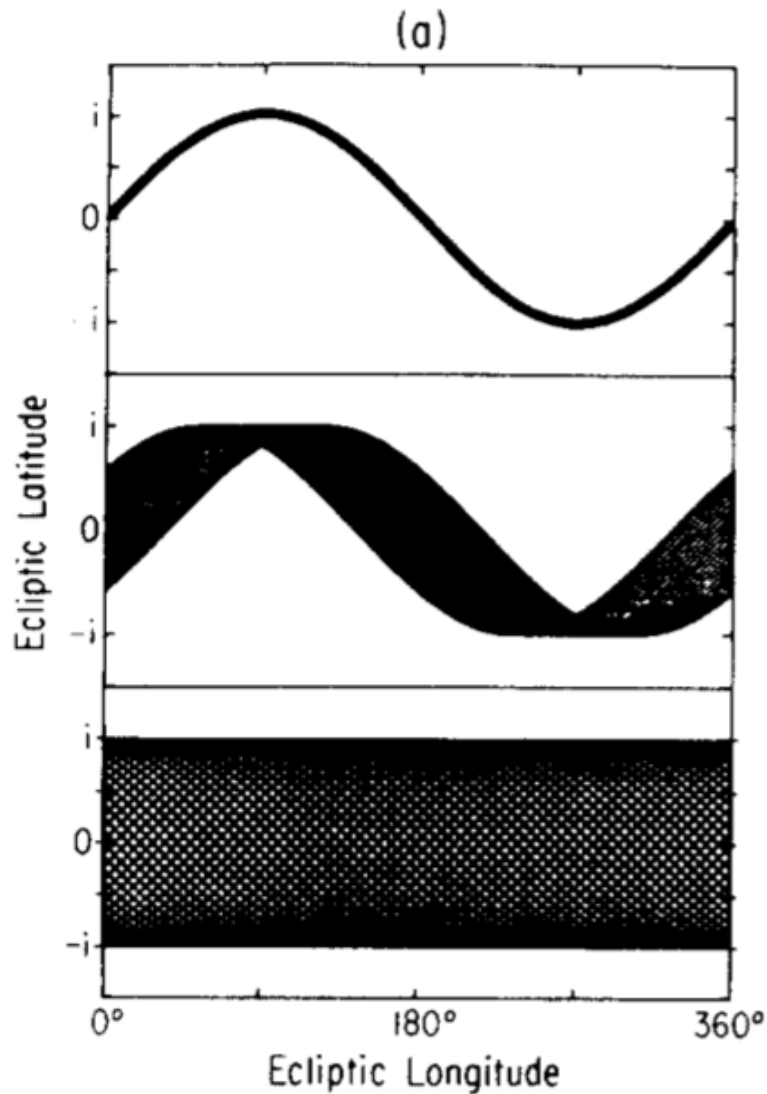


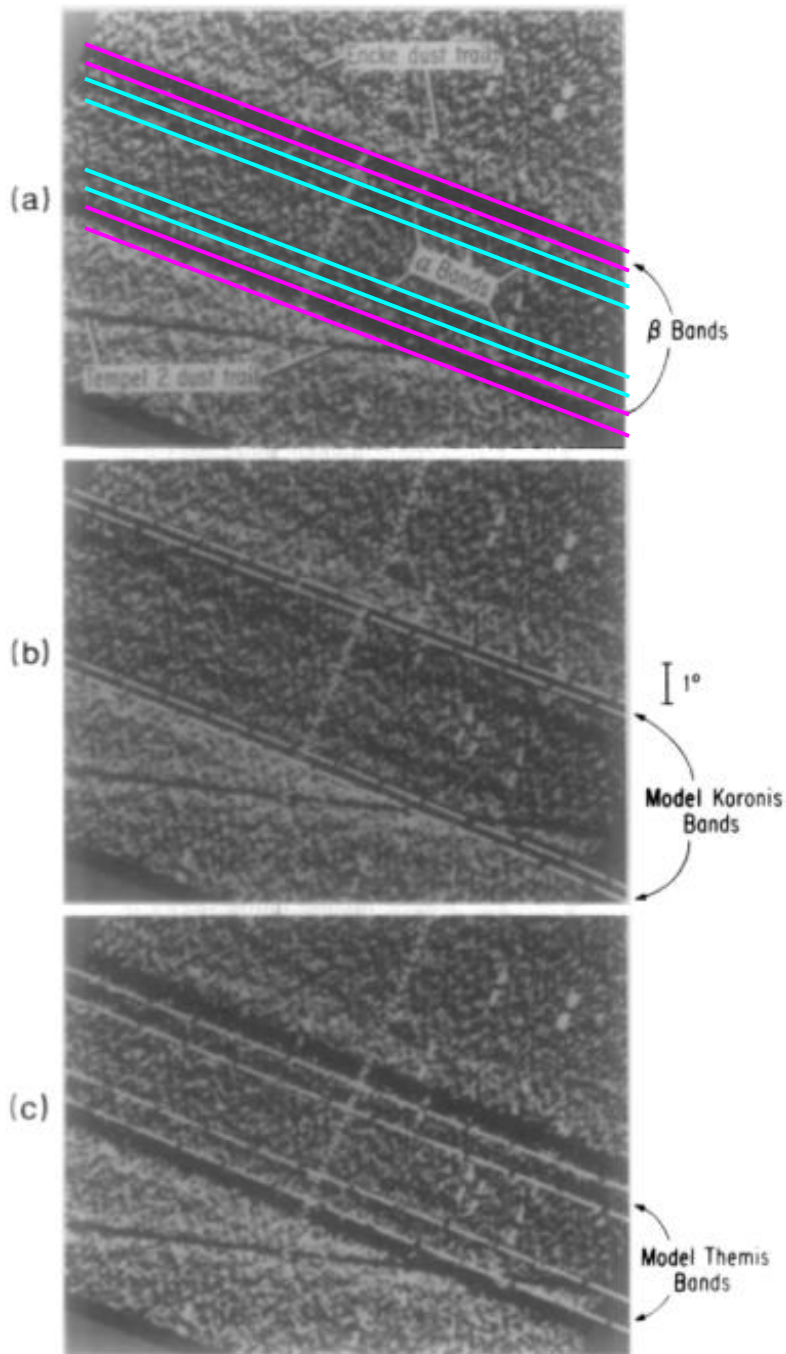
$\Omega(^{\circ})$	$i(^{\circ})$	Method	Position	References
$87 \pm 4$	$3.0 \pm 0.3$	Optical	0.3-1.0AU	1
$\sim 80$	$\sim 2$	Optical	$\approx 1$ AU	2
38-61	$1.5 \pm 0.1$	Infrared, Latitude of peak flux	$\geq 1$ AU	3
$75 \pm 2$	1.8-2.4	Infrared, Pole brightness	1AU	3
$77.7 \pm 0.6$	$2.03 \pm 0.017$	Infrared brightness fitting	$\approx 1$ AU	4
$99.9 \pm 7.8$	$1.16 \pm 0.09$	Infrared, latitude of dust bands' midpoint	2-3	5

Venus  $i=3.4^{\circ}$   $\Omega=77^{\circ}$   
Mars  $i=1.9^{\circ}$   $\Omega=50^{\circ}$   
Jupiter  $i=1.3^{\circ}$   $\Omega=101^{\circ}$   
Saturn  $i=2.5^{\circ}$   $\Omega=114^{\circ}$

**Table 1.** Plane of symmetry of the zodiacal cloud. References: 1) Leinert et al. (1980), 2) Kwon et al. (2004), 3) Kwon and Hong (1998), 4) Kelsall et al. (1998), 5) Grogan et al. 2001

# How to form the band-structure

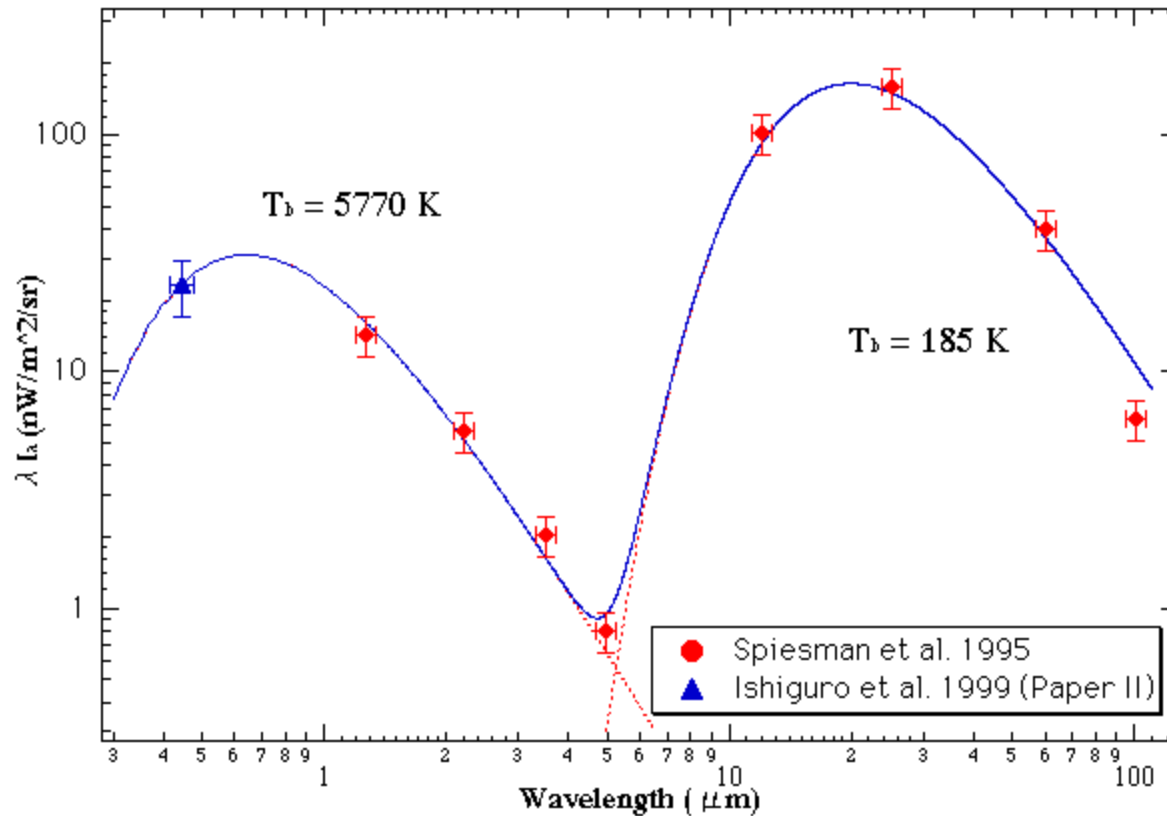




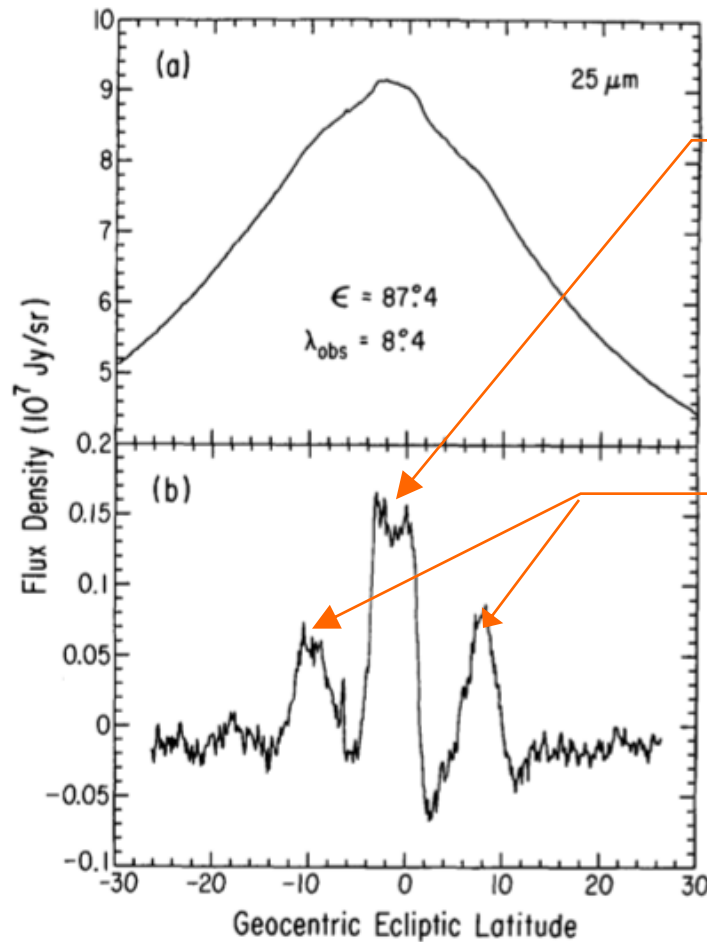
Sykes 1990, Icarus 85, 267-289.

FIG. 8. (a) An IRAS skyflux map (Plate 95, 25  $\mu\text{m}$ ) has been boxcar high-pass filtered, using a filter width of  $1^\circ$  along the scan direction, allowing the  $\alpha$  and  $\beta$  bands to be much more easily distinguished than when using unfiltered images. The edges of model (b) Koronis and (c) Themis dust bands are then projected onto the skyflux map for comparison with the observed bands. No differences in the comparisons between these and unfiltered images are seen.

# Spectrum of dust band



# Interplanetary dust bands: Their relation to asteroid families



Themis/Koronis

Eos

FIG. 1. (a) A scan of the ecliptic at 25  $\mu$ m averaged over  $1/8^\circ$  in the scan direction (along a line of constant longitude, near the ecliptic) and  $1/2^\circ$  in the cross-scan direction. The solar elongation ( $\epsilon$ ) is the Sun–Earth observation angle.  $\lambda_{\text{OBS}}$  is the geocentric ecliptic longitude of observation. (b) The latitudinal profile has been zero-sum high-pass filtered using a filter width of  $3.5$  to suppress the broad zodiacal background and enhance the dust bands. Three prominent bands are apparent, and the central band is seen to split.

# GROUPS OF ASTEROIDS PROBABLY OF COMMON ORIGIN,

BY KIYOTSUGU HIRAYAMA.

On examining the distributions of the asteroids with respect to their orbital elements, particularly to the mean motion ( $n$ ), the inclination ( $i$ ) and the eccentricity ( $e$ ), we notice condensations here and there. In general, they seem to be due to chance. But there are some which are too conspicuous to be accounted for by the laws of probability alone.

As an example of such peculiar groups, I shall take the condensation near  $n = 730''$ . Out of 790 orbits given in the *Berliner Jahrbuch* for 1917, taking 37 between  $720''$  and  $740''$  of the mean motion, and classifying them according to the inclination, we count as follows:—

$i$	Actual No.	Total	Prop. No.	Diff.	Corr.
$0^\circ - 4^\circ$	16	149	7	+9	
$4 - 8$	6	213	10	-4	
$8 - 12$	6	194	9	-3	
$12 - 16$	6	131	6	0	
$16 - 20$	3	55	3	0	
$20 -$	0	48	2	-2	
Sum	37	790	37	0	

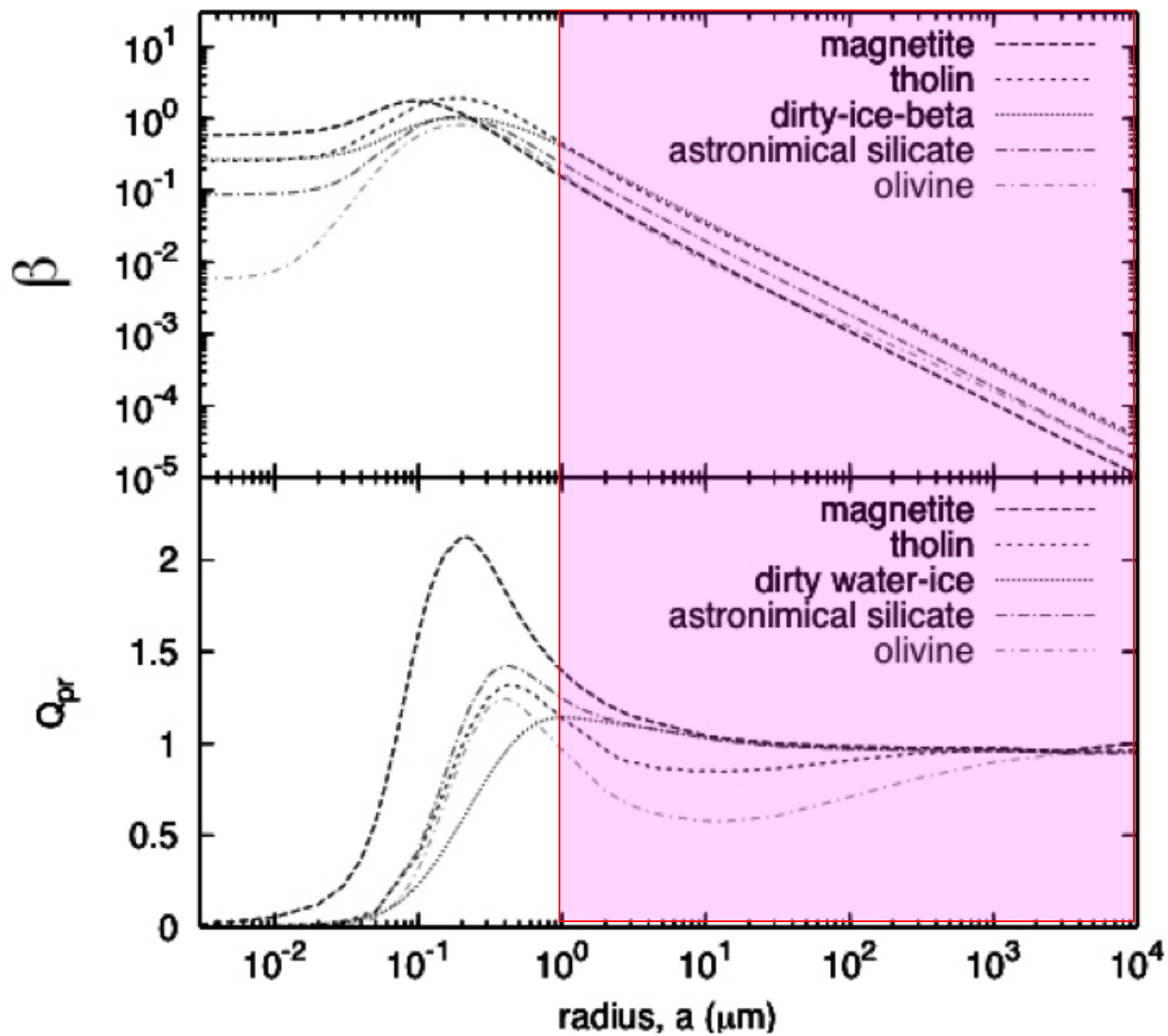
Sixteen orbits between  $0^\circ$  and  $4^\circ$  of  $i$  are surely out of proportion. Assuming the existence of a group physically connected and computing the proportional number according to the remaining  $37 - 16 = 21$ , we see that the probable number of the asteroids belonging to the group is eleven.

Classifying then the sixteen asteroids by the angle of eccentricity ( $\varphi$ ), we get

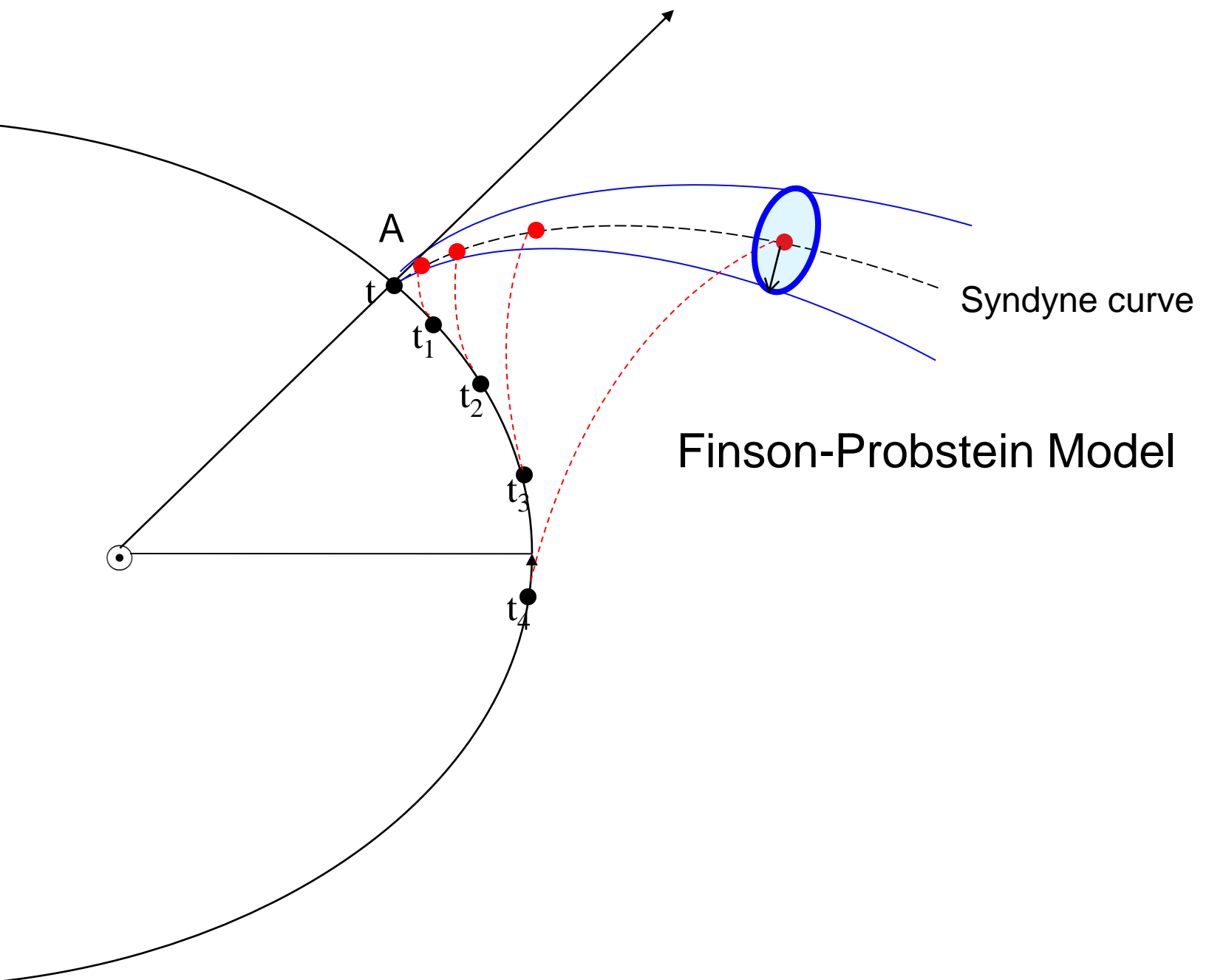
$\varphi$	Actual No.	Total	Prop. No.	Diff.
$0^\circ - 4^\circ$	10	123	2	+8
$4 - 8$	4	263	5	-1
$8 - 12$	1	235	5	-4

Referring to the theory which will be mentioned below, there can be little doubt about the physical relation connecting these asteroids. So I venture to name the group the *Koronis Family*, associating the name of the asteroid (158) which was discovered first.

I find two more families which will be named the *Eos* (221) *Family* and the *Themis* (24) *Family*. The first contains 19 asteroids within the limits



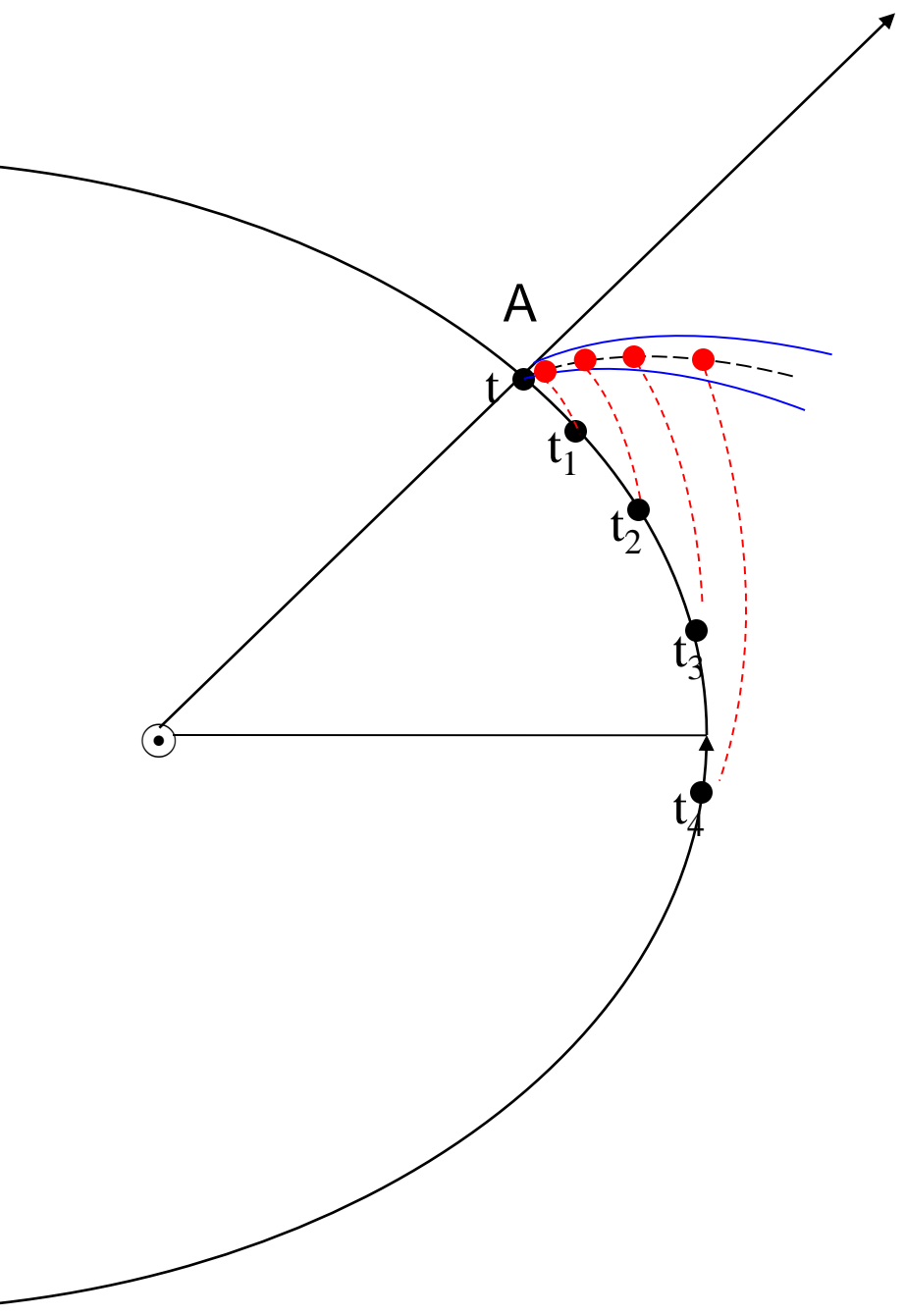
Small Particles ( $a \sim 0.5 \mu\text{m}$ ): unbound orbit



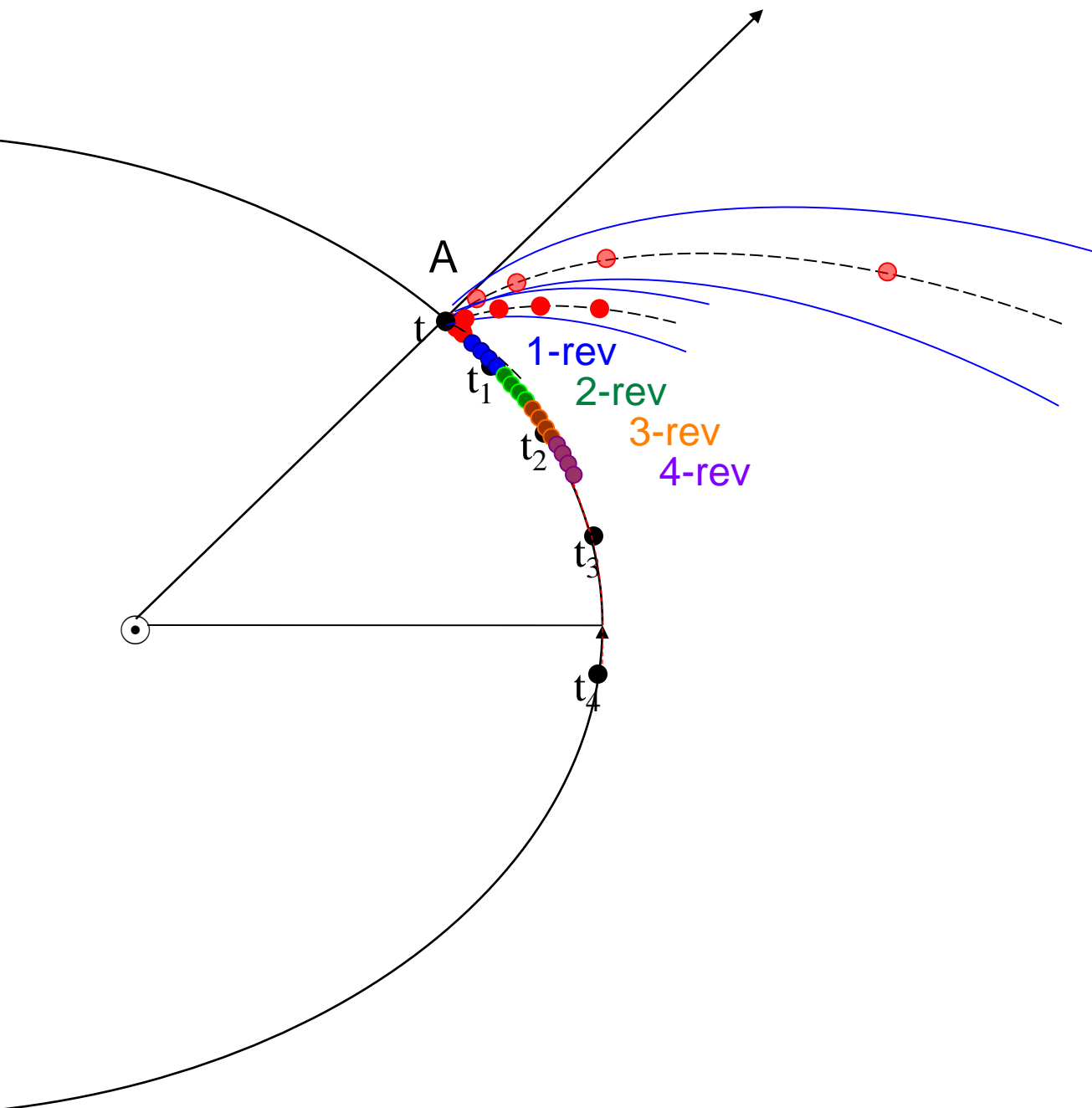
Finson-Probstein Model

Syndyne curve

# Medium-Size Particles ( $a=10\sim 100\mu\text{m}$ ): bound orbit



# Large Particles ( $a \sim 1\text{mm}$ ): bound orbit and embedded in coma



# What is 'neckline'

- Neck-line structure is temporary brightness enhancement by the particles ejected at the point  $180^\circ$  away in true anomaly from the observed point (Kimura & Liu, 1977). Before the perihelion, dust particles are initially ejected isotropically from the nucleus, but after perihelion they collapse onto the orbital plane of the parent comet around the second node, and become ellipsoidal. As a result, the shell looks like a narrow, extended ("Neck Line") structure when the Earth is close to the comet's orbital plane.

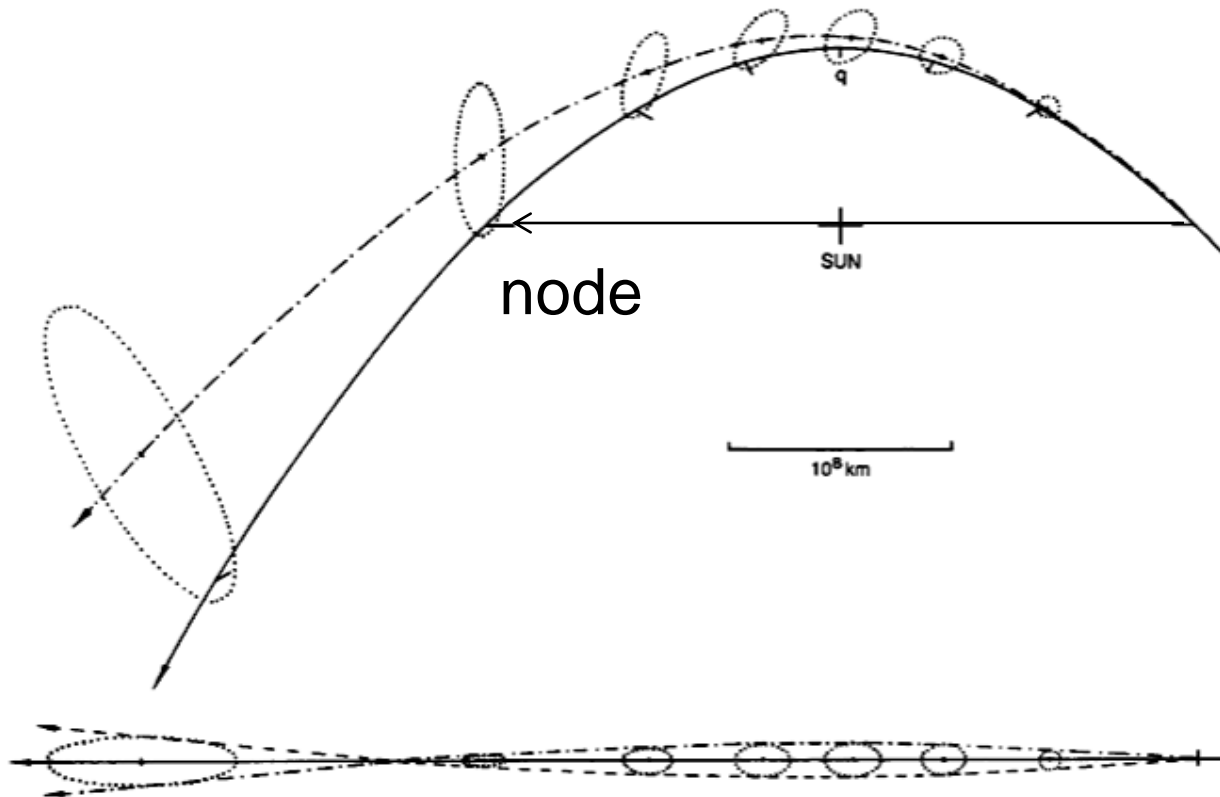
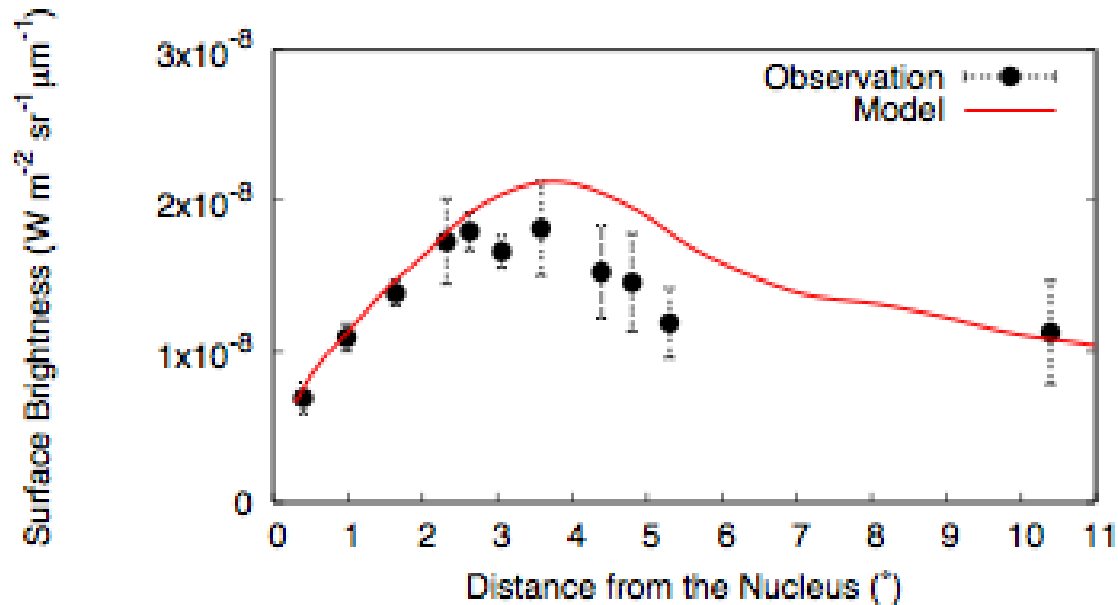


FIG. 1. Time evolution of an isotropic dust shell ejected from the inner coma of Comet Bennett 1970II at the anomaly of  $-90^\circ$  with a radial velocity of  $2 \text{ km sec}^{-1}$ . In the upper part the line of sight is perpendicular to the comet orbit plane; in the lower part this plane is seen edgewise. The dust is characterized by  $1 - \mu = 0.1$ . The solid line is the orbit of the comet nucleus, the dashed and dashed-and-dotted lines are the orbits of the dust grains ejected perpendicularly to the comet orbit plane.

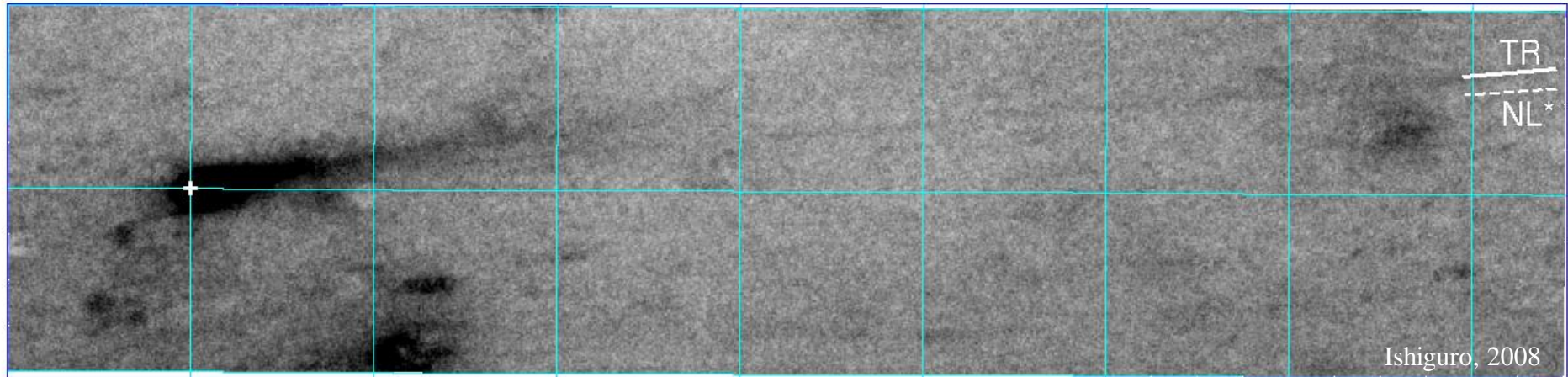
QuickTime™ and a  
decompressor  
are needed to see this picture.

# Surface Brightness of 4P/Faye dust trail



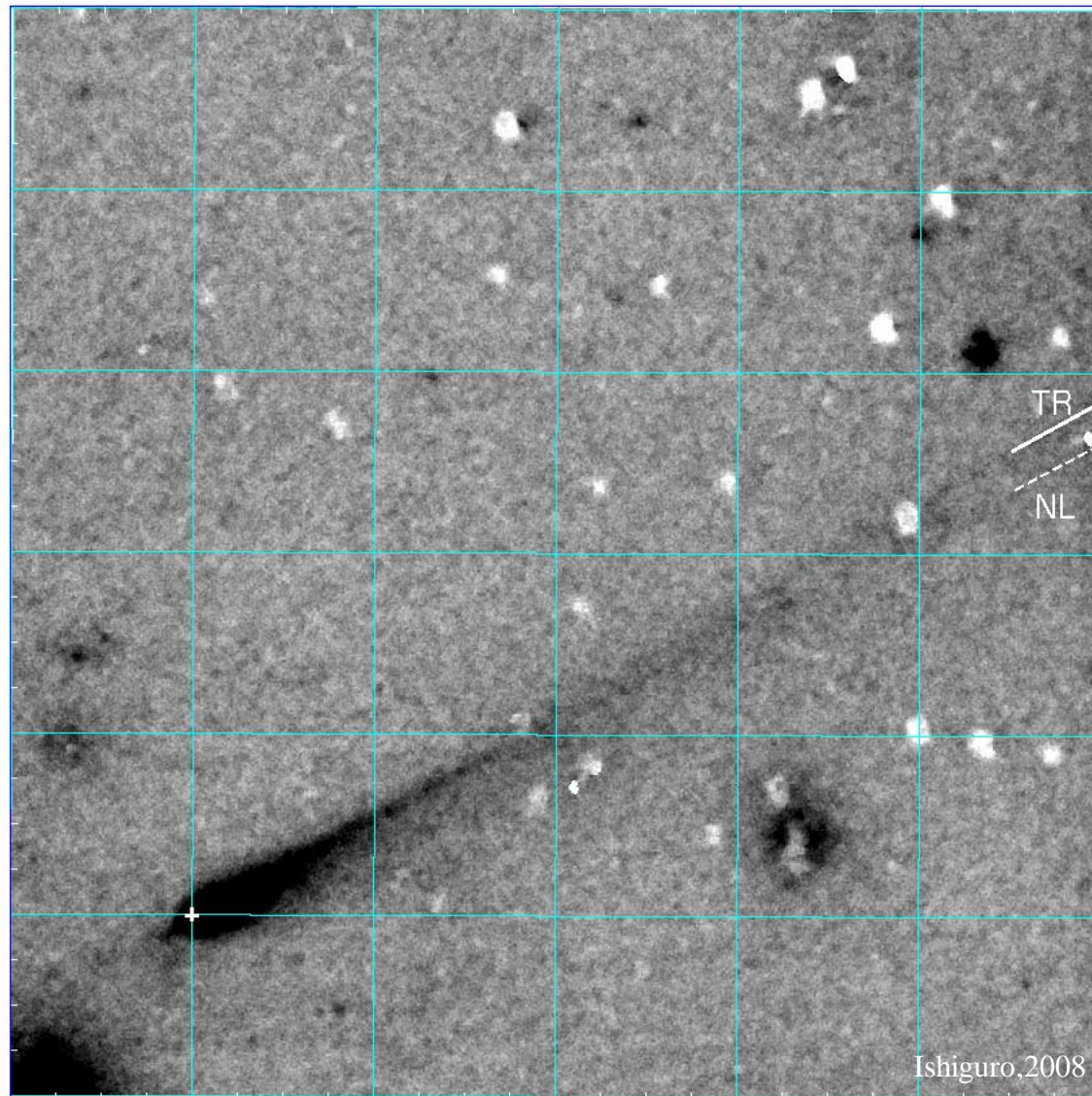
Sarugaku et al. 2007

# Comet 67P/Churyumov-Gerasimenko



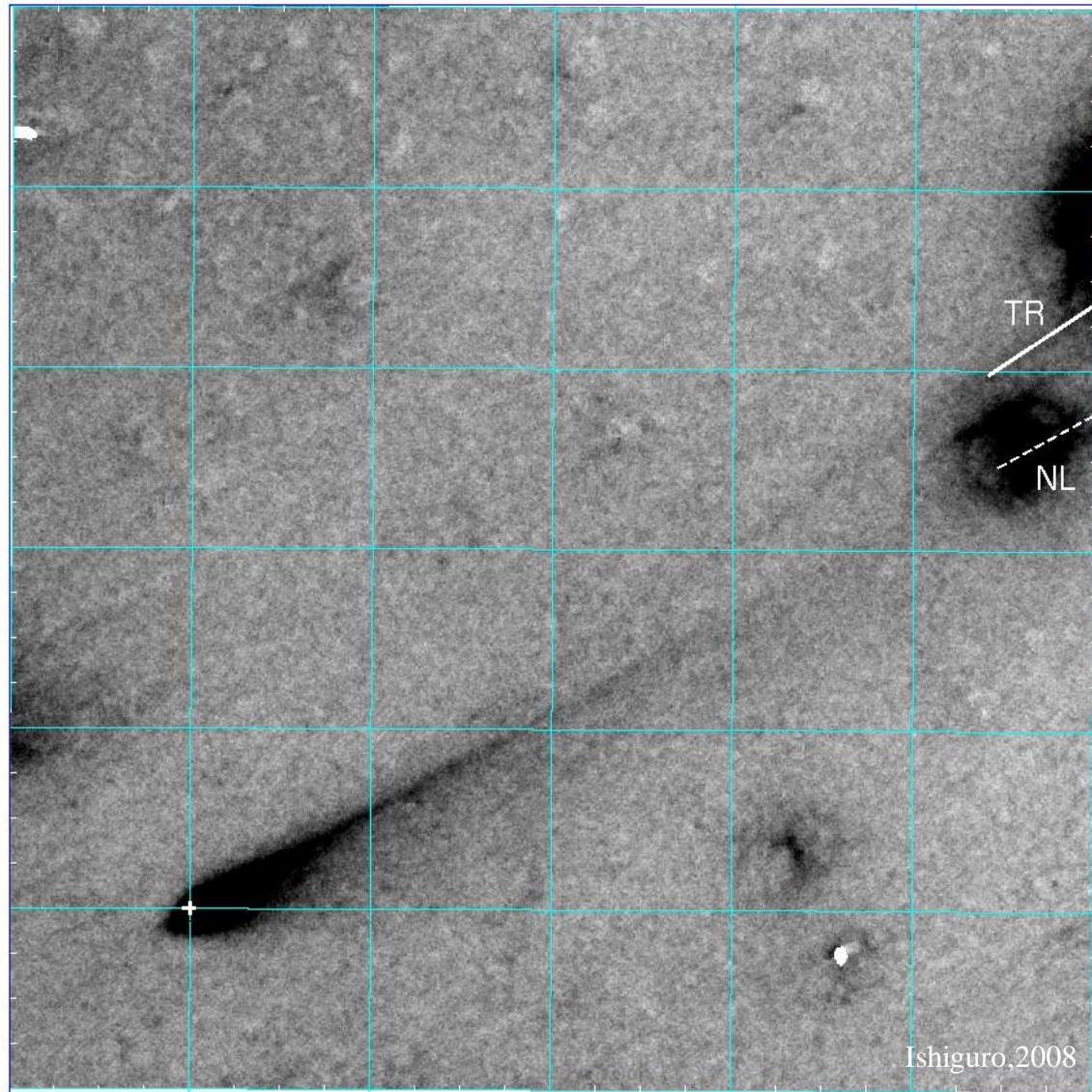
2002/09/09  
(23 days after the perihelion)

# Comet 67P/Churyumov-Gerasimenko



2002/12/02  
(107 days after the perihelion)

# Comet 67P/Churyumov-Gerasimenko



2003/02/01  
(168 days after the perihelion)

$a_{MAX} = 5 \text{ cm}$

(a)

$a_{MAX} = 5 \text{ mm}$

(b)

$a_{MAX} = 500 \mu\text{m}$

(c)

(d)

(e)

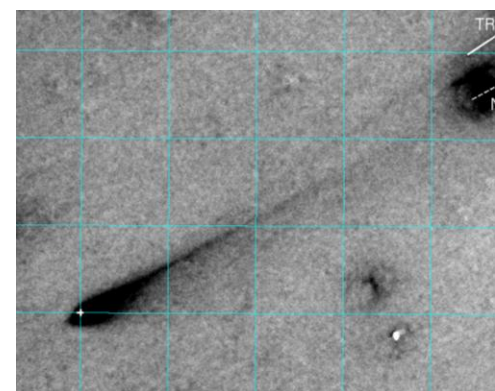
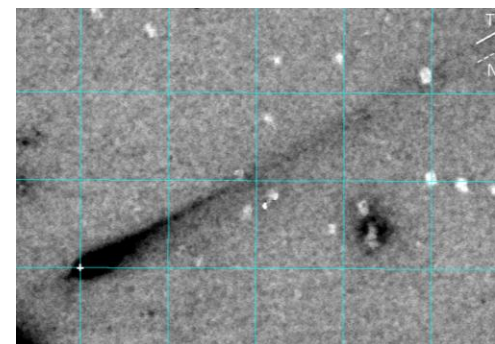
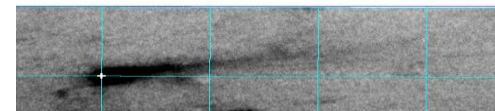
(f)

(g)

(h)

(i)

$q = -3.5 \quad k = 3 \quad V_0 = 3 \text{ m/s}$



$V_0=3 \text{ m s}^{-1}$

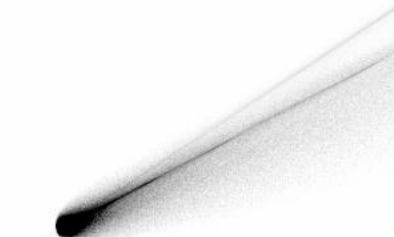
(a)



(d)



(g)

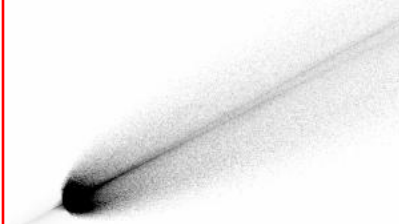


$V_0=6 \text{ m s}^{-1}$

(b)



(e)



(h)



$V_0=9 \text{ m s}^{-1}$

(c)



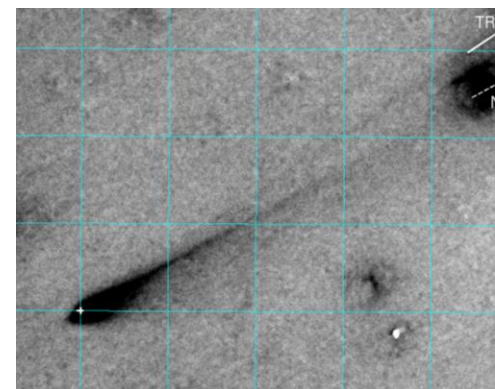
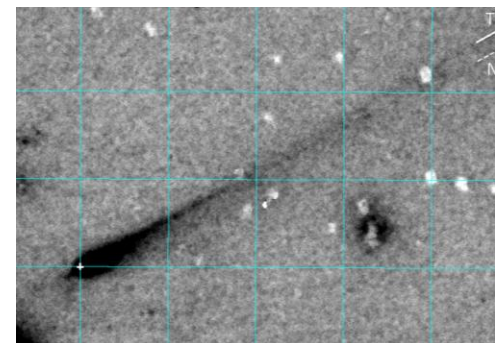
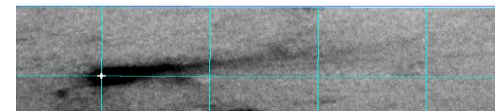
(f)



(i)



$a_{MAX}=5\text{mm}$   $q=-3.5$   $k=3$



$q = -3.0$

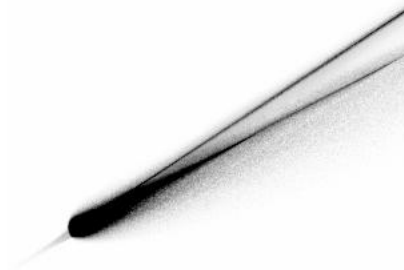
(a)



(d)



(g)



$q = -3.5$

(b)



(e)



(h)



$q = -4.0$

(c)



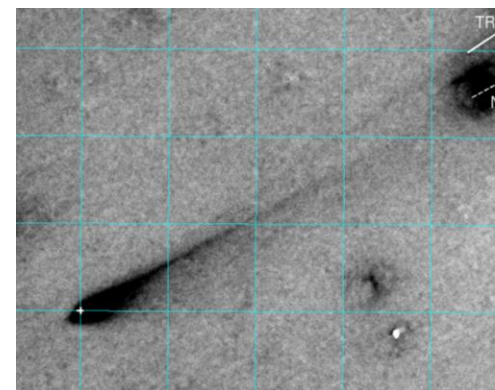
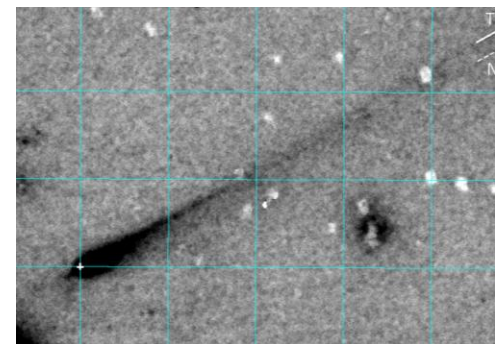
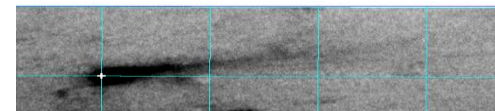
(f)



(i)



$a_{MAX} = 5\text{mm}$   $Vo = 3\text{m/s}$   $k = 3$



# Discovery of Interplanetary Dust Bands

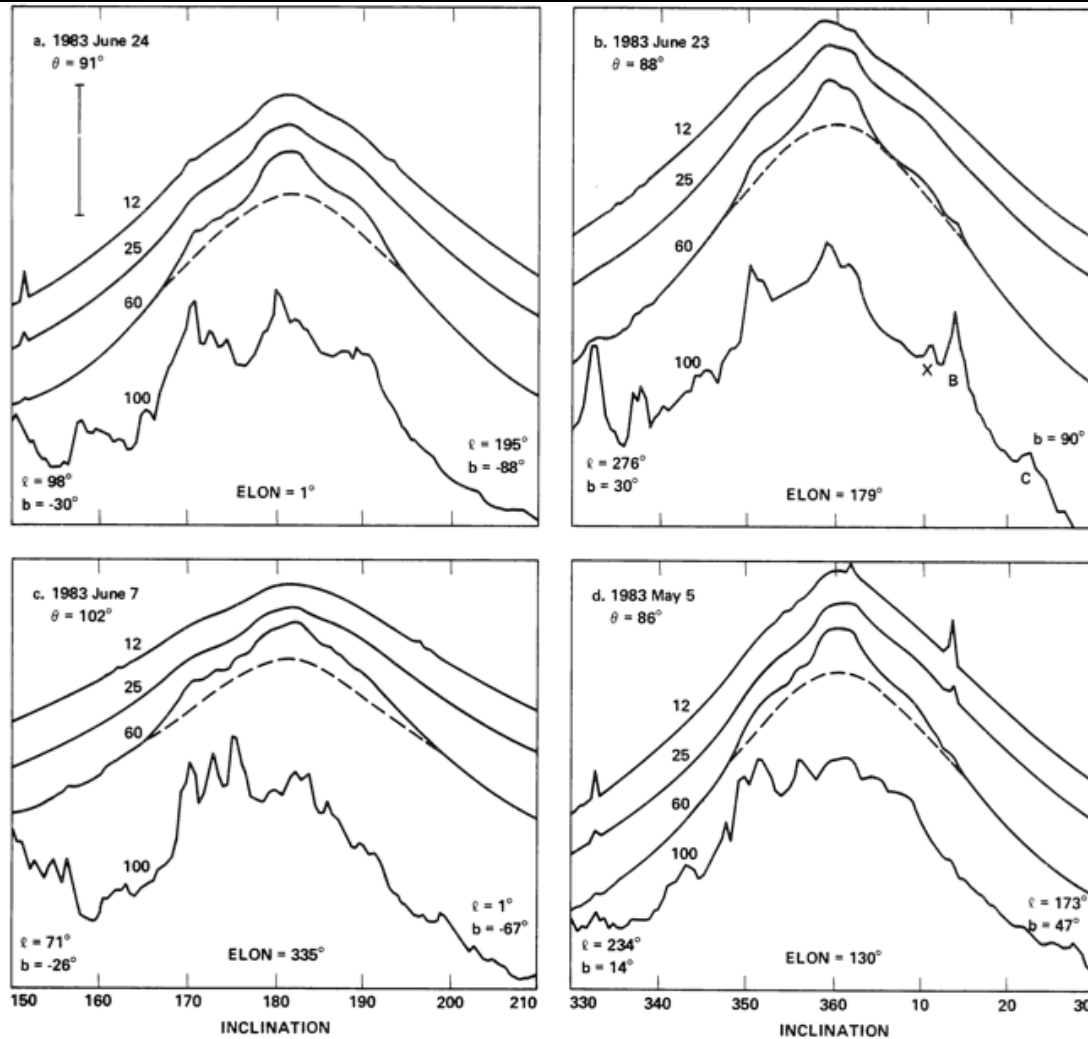


FIG. 2.—Half-degree beam scans crossing the ecliptic at four different longitudes (ELON), showing “mesa” and “shoulder” structures in the four wavelength bands. The scans have been suppressed by arbitrary amounts. Dashed curves representing the smooth component of the zodiacal emission at 60  $\mu\text{m}$  are included for illustration only; detailed modeling has not been performed. The parameter  $\theta$  is the constant angle from the Sun vector; inclination measures the rotation about that vector. The ecliptic is at inclinations  $0^\circ$  and  $180^\circ$ . The ends of the depicted portions of the scans are marked with their galactic coordinates. The vertical bar in (a) corresponds to 12, 30, 10, and 6  $\text{MJy sr}^{-1}$  in the four bands, assuming spectra are flat in  $F_\nu$ . The letters labeling 100  $\mu\text{m}$  features in (b) refer to regions discussed in the text.